

MUKESH ARYAL

**EFFECTS OF DZYALOSHINSKII-MORIYA
INTERACTION ON DOMAIN WALL
DYNAMICS IN FERROMAGNETIC
STRIPS**

Science and Engineering
Bachelor Thesis
May 2019

ABSTRACT

Mukesh Aryal: Effects of Dzyaloshinskii-Moriya interaction on domain wall dynamics in ferromagnetic strips
Bachelor's Degree Programme in Science and Engineering
Tampere University
Physics
May 2019

The prime objective of the thesis was to study the effects of interfacial Dzyaloshinskii-Moriya interaction (DMI) on Walker breakdown phenomenon in an ideal ferromagnetic system of uniformly magnetized domains. The system constitutes a single domain wall between the domains.

The study exploited the use of GPU-accelerated micromagnetic simulation program Mumax3 to simulate a physical experiment. The simulated system included two uniformly magnetized domains separated by a Bloch wall. The domain wall was driven by an applied magnetic field. The simulation was performed for a range of DMI values by applying magnetic fields of different magnitudes. The domain wall velocity was then calculated using the domain wall position and elapsed time of the output data file obtained from the simulation. Numerical estimation of Walker breakdown velocity and Walker field was acquired from the domain wall velocity curve. The final outcome of the analysis revealed a linear dependence of Walker field and Walker breakdown on interfacial DMI.

The study also suggested that DMI could influence a system differently depending on its magnitude. A system with a trace magnitude of DMI had a higher delay in the initial propagation of domain wall but a system equipped with a higher magnitude of DMI showed smaller delay in the initial stage of domain wall propagation.

Keywords: Dzyaloshinskii-Moriya interaction, Walker breakdown, magnetic domains, Bloch wall, Walker field

The originality of this thesis has been checked using the Turnitin Originality Check service.

PREFACE

This research work is a part of bachelor's degree program in Science and Engineering at Tampere University. The research has been completed under the supervision of Associate Professor Lasse Laurson.

I would like to express my gratitude to Associate Professor Lasse Laurson for giving me an opportunity to do this research work. His guidance and supervision have made this study possible.

I would also like to thank Tampere University for providing a great platform to learn and explore science. Finally, I would like to thank my colleagues and teachers who have helped and supported me during the time of study.

Tampere, 17 May 2019

Mukesh Aryal

CONTENTS

| | |
|---|----|
| 1.INTRODUCTION..... | 1 |
| 2.THEORETICAL BACKGROUND..... | 2 |
| 2.1 Magnetic Interactions..... | 3 |
| 2.1.1 Exchange Interaction | 3 |
| 2.1.2 Magnetostatic Energy | 4 |
| 2.1.3 Magnetic Anisotropy | 4 |
| 2.2 Magnetic Domains | 4 |
| 2.3 Domain Wall..... | 5 |
| 2.3.1 Bloch Wall..... | 6 |
| 2.3.2 Néel Wall | 6 |
| 2.4 Domain Wall Propagation..... | 7 |
| 2.5 Walker Breakdown | 8 |
| 3.MICROMAGNETIC SIMULATION..... | 10 |
| 3.1 Landua-Lifshitz-Gilbert Equation | 10 |
| 3.2 Simulation Parameters | 10 |
| 3.3 Flowchart | 11 |
| 3.4 Sample Images | 12 |
| 4.RESULT AND DISCUSSION | 14 |
| 5.CONCLUSION | 19 |
| REFERENCES..... | 20 |

LIST OF FIGURES

| | |
|--|-----------|
| <i>Figure 1-a: Model simulated in the project. (Hütner, Herranen et al. 2018)</i> | <i>1</i> |
| <i>Figure 2-a: Creation of magnetic moment as a result of (a) orbital moment and (b) spin moment of an electron (Skomski 2010).....</i> | <i>2</i> |
| <i>Figure 2-b: Magnetic domains in ferromagnetic material formed by the alignment of magnetic dipoles, represented as arrows.</i> | <i>5</i> |
| <i>Figure 2-c: 180° Bloch wall illustrating the transition of magnetic moments, \mathbf{M}_s, inside the wall (Miyazaki, Jin 2012).</i> | <i>6</i> |
| <i>Figure 2-d: Rotation of magnetic moments inside Néel Wall (Miyazaki, Jin 2012).....</i> | <i>7</i> |
| <i>Figure 2-e: Effects of external magnetic field on a system of magnetic domains. External field is represented by H_{ex} in the figure.....</i> | <i>7</i> |
| <i>Figure 2-f: 180° domain wall's velocity as a function of external magnetic field H. Walker field is represented by H_w. (Mougin, Cormier et al. 2007)</i> | <i>9</i> |
| <i>Figure 3-a: Flowchart of the micromagnetic simulation.</i> | <i>11</i> |
| <i>Figure 3-b: Snapshots of moving domain wall for $\mathbf{B} =15\text{mT}$ in the absence of DMI. Elapsed time for each figure is: 1) 0 ns, 2) 0.6 ns, 3) 1.2 ns.....</i> | <i>12</i> |
| <i>Figure 3-c: Snapshots of moving domain wall for $\mathbf{B} =30\text{mT}$ in the presence of 0.2mJm^{-2} DMI. Elapsed time for each figure is: 1) 0 ns, 2) 0.6 ns, 3) 1.2 ns.....</i> | <i>13</i> |
| <i>Figure 4-a: Domain wall velocity against external field under different DMI values. The outcome corresponds to 1) our modelled system, the squares indicate the Walker breakdown velocity, 2) Yoshimura's result for 500nm-wide wire (Yoshimura, Kim et al. 2015). The unit of D (DMI) in both figures is mJm^{-2}.</i> | <i>14</i> |
| <i>Figure 4-b: Relationship between interfacial DMI and 1) Walker field 2) Breakdown velocity.</i> | <i>15</i> |
| <i>Figure 4-c: Domain wall velocity against the external magnetic field for five different DMI values including the anomalous value. The unit of D is mJm^{-2}.</i> | <i>16</i> |
| <i>Figure 4-d: Domain wall velocity against external field for small DMI values, 1) below the anomalous value, 2) above the anomalous value. The unit of D is mJm^{-2}.</i> | <i>16</i> |
| <i>Figure 4-e: Domain wall position against elapsed time in magnetic field $\mathbf{B} = 5.0\text{mT}$ for: 1) smaller values of DMI, 2) higher values of DMI. The unit of D is mJm^{-2}.</i> | <i>17</i> |

LIST OF SYMBOLS AND ABBREVIATIONS

| | |
|---------------------------------|--|
| A | Exchange stiffness |
| \mathbf{B} | Magnetic field |
| \mathbf{d}_{ij} | Dzyaloshinskii – Moriya vector |
| D | Magnitude of Dzyaloshinskii – Moriya interaction |
| DMI | Dzyaloshinskii – Moriya interaction |
| H | Hamiltonian |
| \mathbf{H} | Auxiliary magnetic field |
| H_W | Walker field |
| J | Exchange constant |
| \mathbf{M} | Magnetization |
| M_s | Saturation magnetization |
| m_L | Orbital magnetic moment |
| m_s | Spin magnetic moment |
| $\overrightarrow{\mathbf{M}}_s$ | Magnetic moment |
| $\mathbf{S}_i, \mathbf{S}_j$ | Spins |
| t | Time |
| T | Tesla |
| \mathbf{v} | Velocity |
| α | Gilbert damping parameter |
| μ_0 | Permeability of free space |

1. INTRODUCTION

Magnetic storage devices have been widely used to store digital information in this technological era. Two distinct magnetic polarities opposite to each other are represented as binary bits, 0 and 1, in such devices. Numerous efforts have been made to increase the capability and data retrieval rate in memory devices. The high-speed storage devices that are used today are the results of those endeavours. In the process of improving the speed of magnetic storage devices, researchers have uncovered a particular interaction called *Dzyaloshinskii-Moriya interaction* that has been found to influence the stability of *domain walls*.

The objective of this project is to study the effect of Dzyaloshinskii-Moriya interaction, abbreviated as *DMI*, on the dynamics of the domain wall in a ferromagnetic strip. The strip consists of two uniformly magnetized domains separated by a *Bloch wall*. The project exploits the use of computer simulations to replicate a physical experiment.

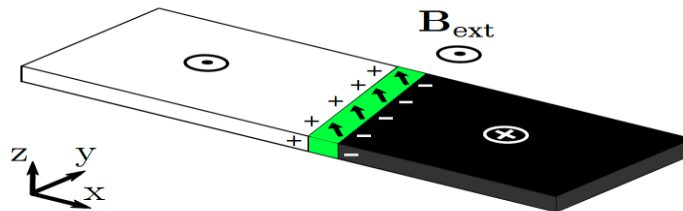


Figure 1-a: Model simulated in the project. (Hütner, Herranen et al. 2018)

Figure 1-a demonstrates the schematics of the simulation used in the project. The pluses and minuses in the figure represent the magnetic charges emerged due to the tilt of the domain wall. The domain wall, separating two uniformly magnetic regions, is a pure *Bloch wall* in equilibrium. The domain wall starts to propagate under the influence of external magnetic field and attains a different steady state resembling a partial *Néel wall*. This causes magnetic charges to surface in the adjoining regions of the domain wall.

The stability of the domain walls can be investigated by observing a phenomenon called *Walker breakdown*. In figure 1-a, Walker breakdown occurs when the magnetization within the domain wall, represented as arrows, starts precessing. The project studies the relationship between DMI and Walker breakdown within a fixed range of DMI values and reports on the findings based on the simulation.

2. THEORETICAL BACKGROUND

Magnetism is associated with charged particles. When charged particles move, they change magnetic fields around them and give rise to magnetism. Magnets can best be described using the concept of *magnetic dipole*. Any revolving charge or a charge spinning around its axis can be considered as a magnetic dipole. The strength of the magnetic dipole to align itself with external magnetic field is called *magnetic dipole moment* or simply *magnetic moment*. (magnetism 2019.) A figure illustrating the origin of magnetic moment is given in figure 2-a.

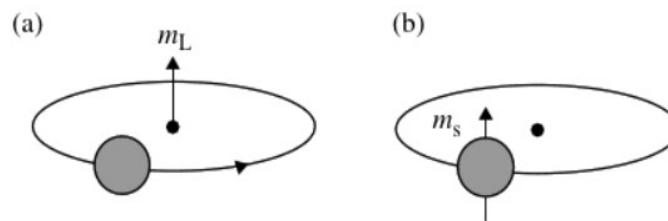


Figure 2-a: Creation of magnetic moment as a result of (a) orbital moment and (b) spin moment of an electron (Skomski 2010).

Magnetism in solids can be argued to originate solely due to the motion of electrons (Skomski 2010). Magnetic dipole in an atom, arising from the spin and movement of the electron, can either nullify each other or add up to create a net dipole moment. An atom with a net dipole moment is analogous to a tiny magnet with magnetic fields around it. A material consisting of such atoms shows strong magnetic properties. One such category of material which exhibits strong magnetic property is ferromagnetic material. Common examples of ferromagnetic materials are iron, cobalt and nickel. The mechanism involving the interaction of ferromagnetic material is called ferromagnetism. It is a very strong property and is associated with materials having permanent magnetic moment.

To understand the regime of magnetism within the scope of this thesis, it is necessary to get familiar with concepts like magnetic interactions, magnetic domain, domain wall, and Walker breakdown.

2.1 Magnetic Interactions

The internal energy of a ferromagnet is affected by different interactions. The interactions can be either local or non-local. Local interactions only depend on the values of local magnetization while non-local interactions depend on the magnetization of every point in the sample. Interactions from the exchange energy, anisotropy energy, external magnetic field and magnetoelastic contributions are all local. On the contrary, contributions from stray field and magnetostrictive term belong to non-local interactions. Exchange interactions, magnetostatic energy, and magnetic anisotropy are very important concepts when discussing magnetic domains and domain walls; therefore, they are discussed more in detail.

2.1.1 Exchange Interaction

Electrons are fermions and they are indistinguishable. Exchange interaction is a consequence of quantum mechanical effects on the electrons. It has two contributions, symmetric exchange that includes the Heisenberg term, and antisymmetric exchange that includes the *Dzyaloshinskii-Moriya* term. The symmetric exchange between two neighbouring spins, S_i and S_j , can be explained using a Hamiltonian, an operator related to the total energy of the system. It supports parallel or antiparallel alignment of the spins and is expressed as

$$H = -2J\mathbf{S}_i \cdot \mathbf{S}_j \quad (1)$$

where H is the Hamiltonian and J is the exchange constant which is a measure of the interaction intensity. (Guimarães 2017.)

The antisymmetric exchange interaction is also known as the Dzyaloshinskii – Moriya interaction. It favours canted arrangement of the spins. Its expression is given by

$$H = \mathbf{d}_{ij} \cdot (\mathbf{S}_i \times \mathbf{S}_j) \quad (2)$$

where \mathbf{d}_{ij} is the Dzyaloshinskii – Moriya vector and its modulus gives the intensity of the interaction. This interaction is present in bulk materials whose unit cell does not have inversion symmetry. It is also present at an interface of a material due to the broken symmetry. The antisymmetric exchange at an interface is also called interfacial Dzyaloshinskii – Moriya interaction. The exchange energy is proportional to the square of the gradient of the magnetization; thus, its terms measure the nonuniformity of the magnetization in the sample. (Guimarães 2017.)

2.1.2 Magnetostatic Energy

The magnetic potential energy produced when keeping a magnetic body in a magnetic field is called magnetostatic energy. In the case of strong magnetic body, magnetostatic energy can be generated even in the absence of external magnetic field. It exists because of the internal magnetic field existing in the opposite direction from the magnetization. Such field within a magnet is called demagnetizing field which arises from the divergence of the magnetization. The expression for magnetostatic energy arising from the energy of magnetization in the demagnetizing field is given by

$$E_{ms} = -\frac{1}{2}\mu_0 \iiint \mathbf{H}_d \cdot \mathbf{M} dV \quad (3)$$

where E_{ms} is the magnetostatic energy, \mathbf{H}_d is the demagnetizing field, \mathbf{M} is the magnetization, and μ_0 is the permeability of free space. The integral is taken over the volume of the sample V . (Guimarães 2017.)

2.1.3 Magnetic Anisotropy

Magnetic anisotropy is defined as the dependence of material's magnetic properties, especially energy, on the relative direction of magnetization and structural axes. It originates from factors like shape of the material, stress in the material, atomic segregation, and others. In simple cases, matter chooses an axis along which energy is at minimum. Such axis is referred to as an easy axis. (Guimarães 2017.)

Different materials can have different kinds of magnetic anisotropy. Some of the common magnetic anisotropies are uniaxial, triaxial and cubic. A magnetic particle having uniaxial anisotropy has only one easy axis. The anisotropy energy of such a system can be expressed as

$$E = KV \sin^2 \theta \quad (4)$$

where V is the volume, K is the anisotropy constant, and θ is the angle between the easy axis and the particle's magnetization. The system of interest in this project has uniaxial anisotropy; therefore, only it has been discussed here.

2.2 Magnetic Domains

Landau and Lifshitz founded the domain theory of magnetism in 1935. The theory is based on the assumption that the constituents of a magnetic body are magnetic domains and domain walls between them. (Miyazaki, Jin 2012.) Ferromagnetic materials contain smaller segments inside them where atoms align themselves parallel to each other creating an area having strong magnetization. Such areas are called magnetic domains.

An isolated magnetic body must have minimum free energy at constant temperature in an equilibrium state. Exchange energy and magnetic anisotropy energy of the body are at a minimum whenever the magnetic body reaches magnetization saturation along any easy axis. But the same magnetic charges of the same sign appear on either side surface of the body producing a large demagnetizing field and thus giving rise to large magnetostatic energy. Due to the influence of demagnetizing field, the magnetizations of part of the body switch to other easy directions to reduce the magnetostatic energy. Magnetization along different easy axes results in the formation of magnetic domains. (Miyazaki, Jin 2012.) Figure 2-b shows an example of domains within a ferromagnetic material.

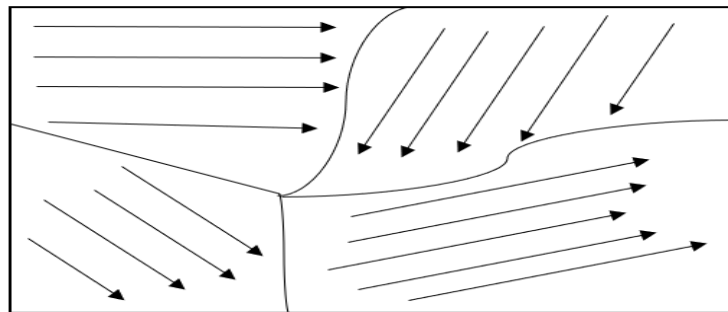


Figure 2-b: *Magnetic domains in ferromagnetic material formed by the alignment of magnetic dipoles, represented as arrows.*

Different magnetic domains can exist inside a ferromagnetic material. In the case of random orientation of domains, ferromagnetic material may still have zero magnetic field strength in spite of being attracted to permanent magnets. Most ferromagnetic materials found in nature like iron, cobalt and nickel are these sorts of materials with no net magnetic field strength. Magnetization is the process of aligning the orientation of those domains by introducing an external magnetic field. Magnetic domains play an important role in magnetism.

2.3 Domain Wall

An interface between two adjoining magnetic domains is called a domain wall. The magnetic moments make a transition from one orientation to another inside the wall. The width of the domain wall depends upon exchange energy and anisotropy energy of the material. The exchange energy is at a minimum when the neighbouring magnetic moments in the wall are as parallel as possible. Under this circumstance, domain wall becomes broad. On the other hand, the anisotropy energy is at the lowest if there are

smaller number of atoms in the wall. Since the requirements for attaining minimum energy with minimum anisotropy energy and minimum exchange energy contradict each other, the domain wall configuration is a compromise between these two energies. (Guimarães 2017.) Mainly, there are two types of domain wall, Bloch Wall and Néel Wall.

2.3.1 Bloch Wall

Consider an infinite plane domain wall with its normal pointing along the x-axis as shown in figure 2-c. The magnetization rotates gradually while shifting from one domain to the neighbouring domain. When there is no magnetic charge in the system to make the magnetostatic energy zero, the magnetic moment distribution in the wall should satisfy the condition that its component normal to the wall remains unchanged along any position x. The domain wall satisfying the above condition is called a Bloch wall. (Miyazaki, Jin 2012.) They are more common in bulk materials.

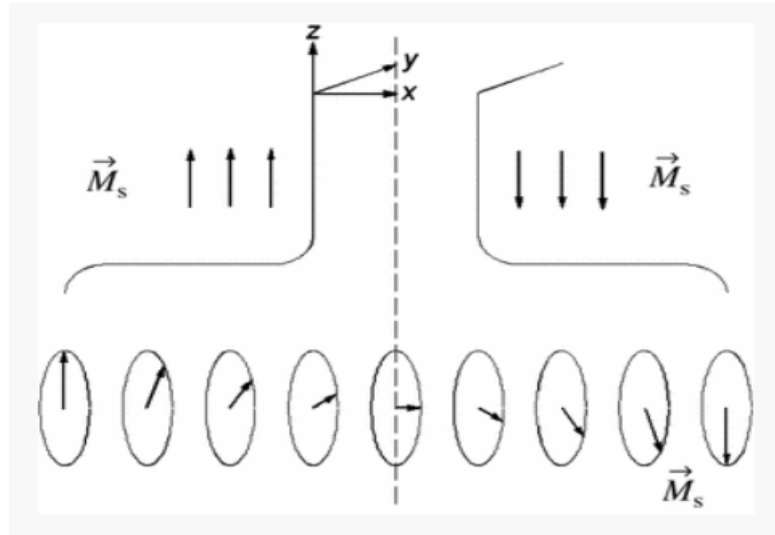


Figure 2-c: 180° Bloch wall illustrating the transition of magnetic moments, \vec{M}_s , inside the wall (Miyazaki, Jin 2012).

2.3.2 Néel Wall

Consider a thin ferromagnetic film. The easy axis of such a film can be in the film plane. The dimension of a Bloch wall normal to the film plane is the thickness of the film. The surface magnetic charges emerge on the belts of intersections of the wall with the film surfaces. Magnetostatic energy contributes to the domain wall energy and its proportion increases with the decrease of film thickness. The domain wall energy, in which the magnetization vector rotates within the film plane with shift of position x, becomes smaller than that of a Bloch wall as the thickness of the film decreases approximately to wall

width. As a result, the former replaces the latter and gives rise to the formation of Néel Wall. (Miyazaki, Jin 2012.) The illustration of Néel Wall is given in figure 2-d.

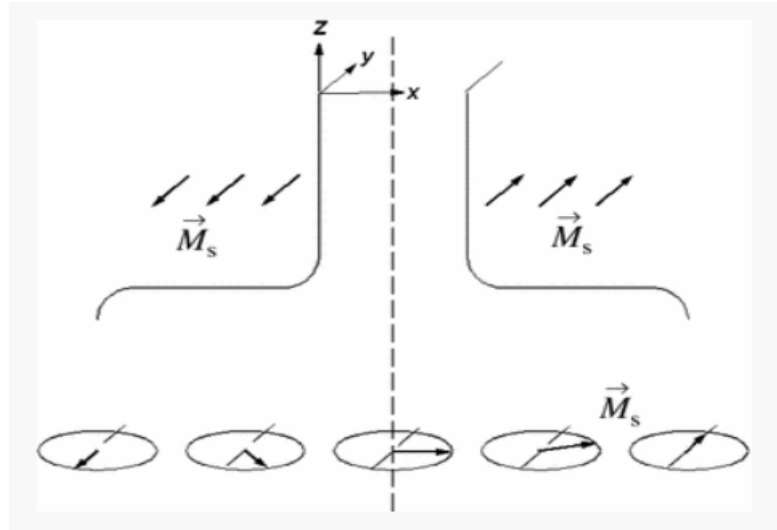


Figure 2-d: Rotation of magnetic moments inside Néel Wall (Miyazaki, Jin 2012).

This wall is more common in very thin films. In contrary to Bloch wall, magnetization in this type of wall rotates in the plane of the domain wall. This type of wall can be stabilized by DMI as well.

2.4 Domain Wall Propagation

When external magnetic field is applied to a system of magnetic domains of different orientation, the field changes the configuration of overall domain structure. The domains aligned closely with the external magnetic field gain energy and other domains, differing from the alignment of external magnetic field, lose energy. The system then tries to minimize its total energy by increasing the size of the favourably oriented domains while decreasing the size of unfavourably oriented domains. (H. Föll 2018.) The domain walls, separating the domains, shift and appear to move during this procedure. The schematics of the phenomenon is portrayed in figure 2-e.

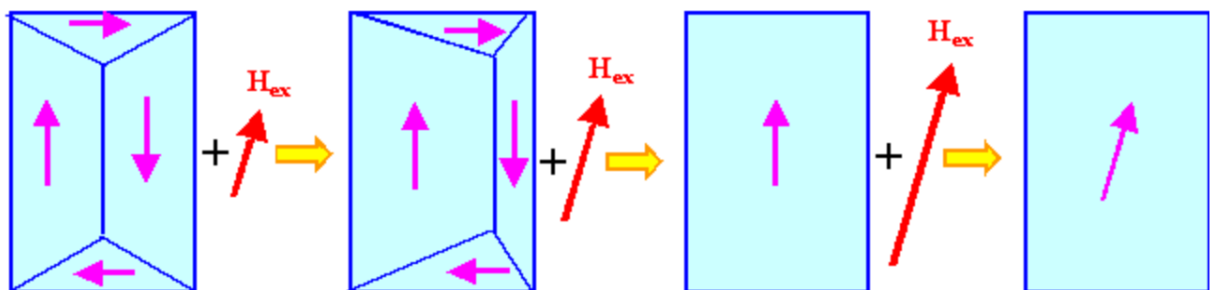


Figure 2-e: Effects of external magnetic field on a system of magnetic domains. External field is represented by H_{ex} in the figure.

Figure 2-e demonstrates the influence of the external field. The external magnetic field increases the size of the favoured magnetic domains while reducing the sizes of unfavoured domains. When the magnitude of external field becomes very high, it results in the formation of single domain having the orientation of the external field as shown in the third stage of figure 2-e. The movement of magnetic domain walls using external field is known as *field-induced domain wall motion*.

The electric current can also be used to move domain walls. Domain wall motion achieved using electric current is known as *current-induced domain wall motion*. An electric current in a ferromagnetic material can give rise to spin polarized electrons. These electrons can transfer angular momentum to the lattice while crossing a magnetic domain wall. This can result in the movement of the domain wall. (Beach, Tsoi et al. 2008.)

2.5 Walker Breakdown

The dynamics of the domain wall contain unique, nonlinear behaviour under the influence of external magnetic field. The domain wall velocity increases linearly with external magnetic field reaching a threshold beyond which it declines abruptly. This phenomenon in field-driven domain wall dynamics is known as *Walker breakdown* and the threshold field value, associated with it, is called *Walker field*. (Yoshimura, Kim et al. 2015.) Walker breakdown occurs due to the onset of precessional domain wall motion that gives rise to a periodic change in the helicity of the wall. As the external field surpasses the Walker field, some part of the energy of the driving field is dissipated in the precessional magnetization dynamics within the wall; as a result, it contributes less to the propagation velocity. Hence, the domain wall velocity is reduced in the process. (Hütner, Herranen et al. 2018.)

Walker breakdown occurs differently in different systems. In a one-dimensional system, corresponding to nanowire geometries, the precession of magnetization is described using a single angular variable. In the case of a two-dimensional system, corresponding to wide enough nanostrip geometries, the instability of the domain wall results because of repeated nucleation and propagation of *Bloch lines* within the wall. Bloch lines are topologically stable magnetization textures corresponding to localized transition regions between different chiralities of Bloch domain wall. (Hütner, Herranen et al. 2018.)

Figure 2-f illustrates the relationship between domain wall propagation and external magnetic field. It shows the behaviour of domain walls before and after the Walker breakdown.

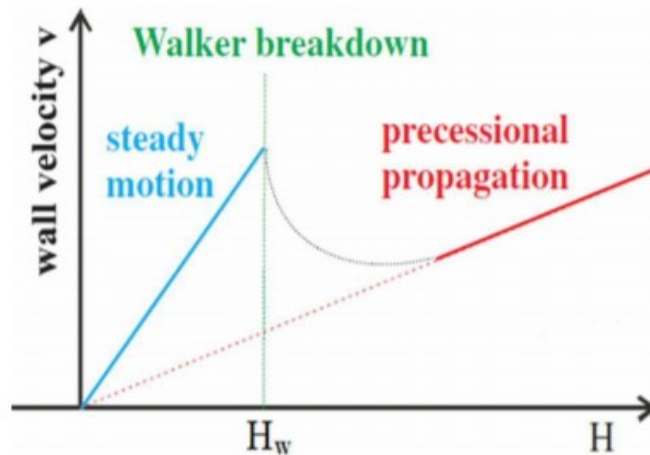


Figure 2-f: 180° domain wall's velocity as a function of external magnetic field H . Walker field is represented by H_w . (Mougin, Cormier et al. 2007)

Figure 2-f shows three different phases of the wall velocity when a 180° domain wall is exposed to external magnetic field. The first phase comprises of steady linear growth of velocity in response to increasing magnetic field up until it reaches the Walker field. Once external field reaches the Walker field, its velocity attains maximum value and starts to reduce immediately afterwards. This particular phenomenon here is called Walker breakdown. As magnetic field grows larger and larger, the propagation velocity again attains a steady linear growth.

3. MICROMAGNETIC SIMULATION

The study of the domain wall dynamics in this project is done through the means of a GPU-accelerated micromagnetic simulation program *MuMax3*. The program solves the space and time-dependent reduced magnetization from the Landau-Lifshitz-Gilbert (LLG) equation. (Vansteenkiste, Leliaert et al. 2014.)

3.1 Landua-Lifshitz-Gilbert Equation

The LLG equation is a differential equation that describes the precessional motion of magnetization in solids. It is named after Lev Landau, Evgeny Lifshitz, and T.L. Gilbert. The LLG equation is an improvement of the original equation of Landau and Lifshitz by Gilbert. The LLG equation is expressed as

$$\frac{\partial \mathbf{M}}{\partial t} = \gamma_G \mathbf{M} \times \mathbf{B}_{eff} + \frac{\alpha}{M_s} \mathbf{M} \times \frac{\partial \mathbf{M}}{\partial t} \quad (5)$$

where \mathbf{M} is the magnetization, M_s is saturation magnetization, γ_G is gyromagnetic-type constant, α is Gilbert damping parameter, t is time, and \mathbf{B}_{eff} is the effective field. The effective field includes the contribution from external magnetic field, magnetostatic field, Heisenberg exchange field and anisotropy field. (Mayergoyz, Bertotti et al. 2008.)

3.2 Simulation Parameters

The material of choice was Co/Ni film with dimension, $1024 \times 512 \times 1.2 \text{ nm}^3$. The system was discretized using a cell of dimension, $2 \times 2 \times 1.2 \text{ nm}^3$. The size of the grid employed in the simulation was $512 \times 256 \times 1$. The material parameters used in the simulations are given in table 3-1.

Table 3-1: Material parameters used in the micromagnetic simulation.

| Quantity | Magntitude |
|--|---------------------------------------|
| Saturation magnetization (M_s) | $8.37 \times 10^5 \text{ Am}^{-1}$ |
| Uniaxial anistropy (K_U) | $1.31 \times 10^6 \text{ Jm}^{-3}$ |
| Exchange stiffness (A) | $1.0 \times 10^{-11} \text{ Jm}^{-1}$ |
| Gilbert damping parameter (α) | 0.15 |

The material parameters used in this project were taken from an article “Soliton-like magnetic domain wall motion induced by the interfacial Dzyaloshinskii-Moriya interaction”. (Yoshimura, Kim et al. 2015.)

3.3 Flowchart

The flowchart of the program that was run to obtain the results is given in figure 3-a.

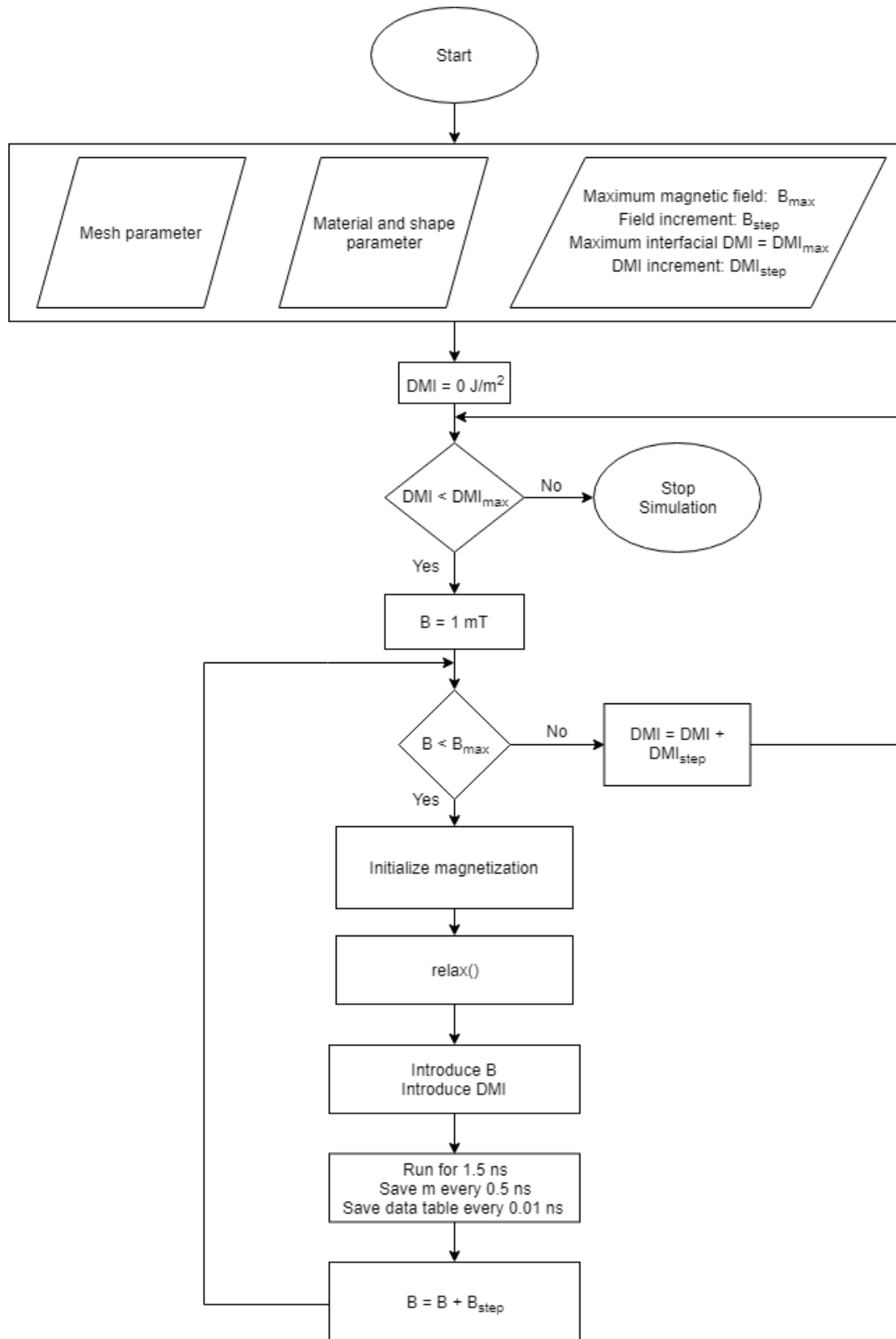


Figure 3-a: Flowchart of the micromagnetic simulation.

The simulation mainly comprised of two confined loops. The function of the loops was to increment the values of interfacial DMI and external magnetic field. The program was run for every 1.5 ns in correspondence to the magnitude of the external magnetic field together with interfacial DMI. The position of the domain wall was then recorded along with the elapsed time.

3.4 Sample Images

The images obtained from the simulation help visualize the process more clearly. The Walker breakdown phenomenon and magnetization orientation is depicted in figure 3-b.

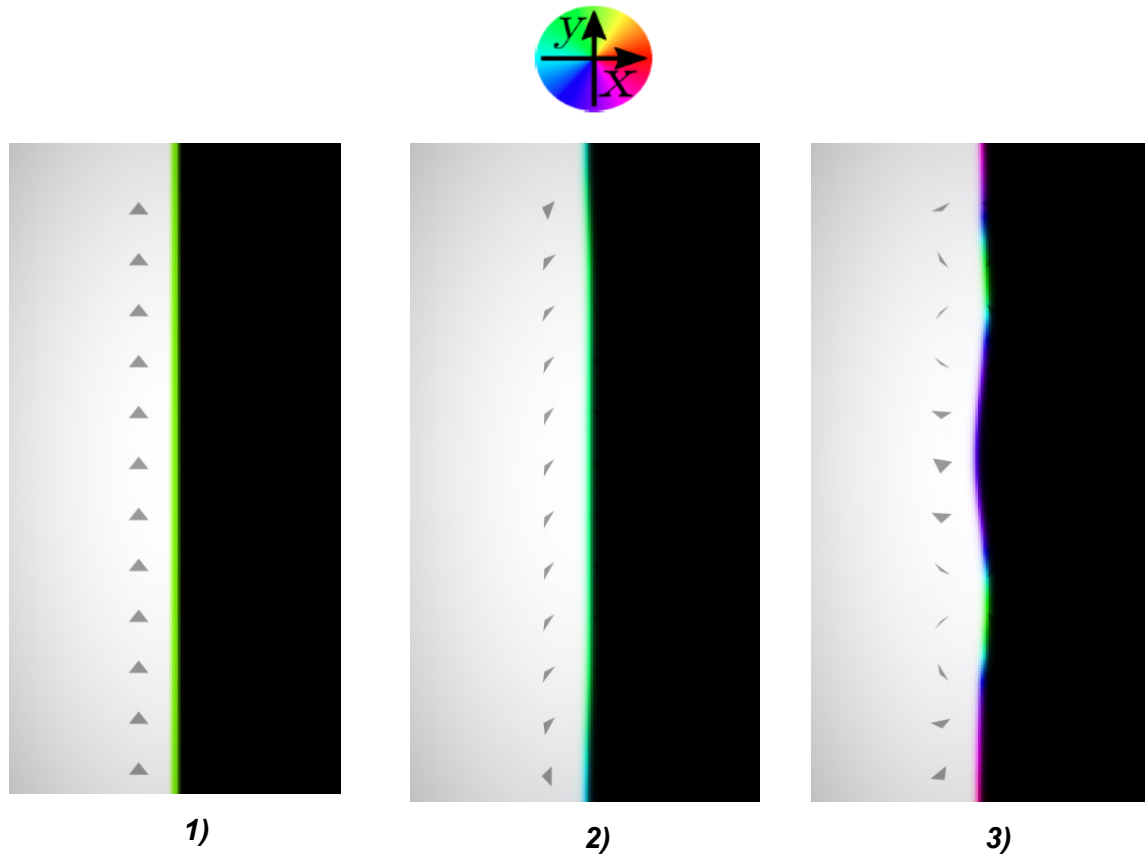


Figure 3-b: Snapshots of moving domain wall for $|B|=15\text{mT}$ in the absence of DMI. Elapsed time for each figure is: 1) 0 ns, 2) 0.6 ns, 3) 1.2 ns.

The snapshots contain different colours to represent different magnetic polarities. The white shade represents magnetic polarities leaving out of the plane and the black colour indicates the magnetic polarities going in to the plane. The arrows represent the direction of magnetic moments engulfed within the domain wall. The colour of the domain wall depends on the orientation of the in-plane magnetic moments forming it. The colour wheel clarifies the representation of different magnetization by different colours. The domain wall in figure 3-b-1 is a pure Bloch wall. As domain wall propagates the domain wall changes into a partial Néel wall as shown in figure 3-b-2. Figure 3-b-3 is a snapshot

of the domain wall after the Walker breakdown. It shows the nucleation of *vertical Bloch lines*.

When DMI is introduced to the system, the magnetization orientation changes differently and the breakdown phenomenon follows different proceedings. Figure 3-c shows different instances of the domain wall under the influence of external field and DMI.

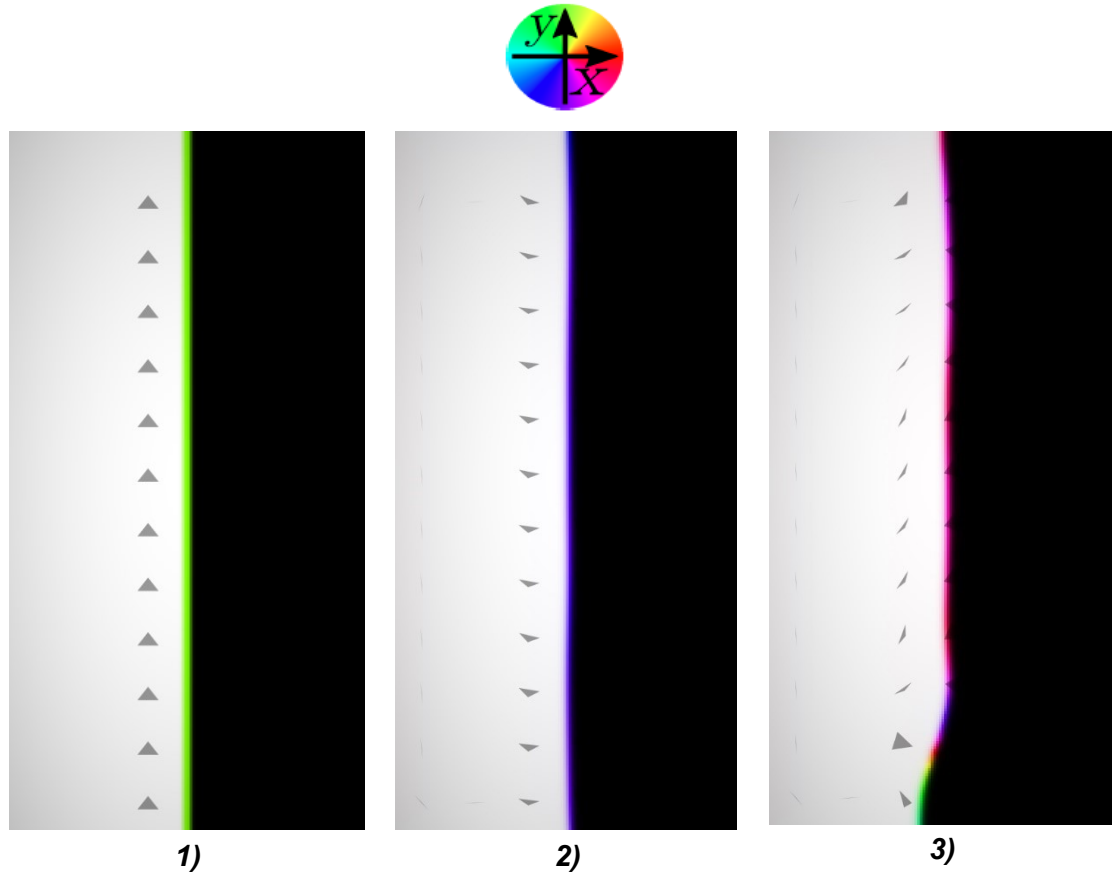


Figure 3-c: Snapshots of moving domain wall for $|B|=30\text{mT}$ in the presence of 0.2mJm^{-2} DMI. Elapsed time for each figure is: 1) 0 ns, 2) 0.6 ns, 3) 1.2 ns.

When DMI is introduced to the system, the system stabilizes to greater extent deferring the process of Walker breakdown. The nucleation of Bloch lines in figure 3-c-3 only initiates in a single place. The intermediate stage, given by figure 3-c-2, shows that the initial magnetization changes drastically during the movement of the domain wall.

4. RESULT AND DISCUSSION

Domain wall velocity for different applied fields was calculated to understand the effect of interfacial DMI on Walker breakdown. Velocity is the rate of change of displacement; therefore, the slope of the domain wall position against elapsed time is the domain wall velocity. The dependence of domain wall velocity on external magnetic field and interfacial DMI is illustrated in figure 4-a-1. The outcome was then compared with the corresponding result of the article on which the simulation parameters were based.

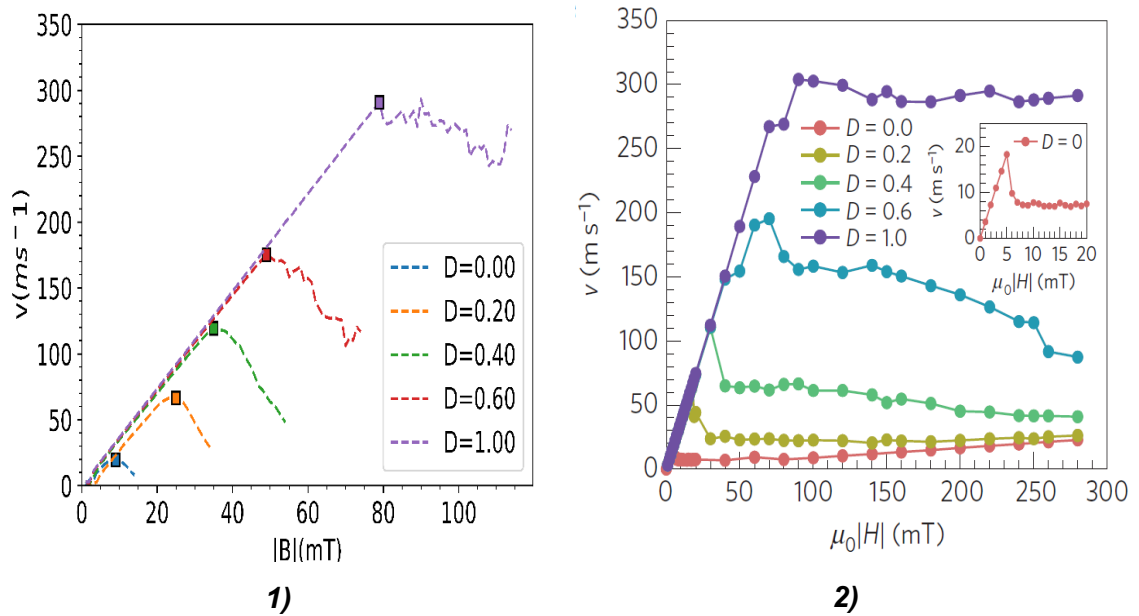


Figure 4-a: Domain wall velocity against external field under different DMI values. The outcome corresponds to 1) our modelled system, the squares indicate the Walker breakdown velocity, 2) Yoshimura's result for 500nm-wide wire (Yoshimura, Kim et al. 2015). The unit of D (DMI) in both figures is mJm^{-2} .

Figure 4-a-1 portrays the influence of DMI on Walker breakdown in our modelled system, a ferromagnetic strip having a cross section of $512 \times 1.2 \text{ nm}^2$. The domain wall velocity begins to decrease abruptly after a period of linear growth. The interest of this research was fixated on Walker breakdown so, the simulation had different range of external field values for every DMI value. The ranges were chosen ensuring that the Walker breakdown would arise at some point within the selected range. Figure-4-a-2 delineates the same effect of interfacial DMI on a 500nm-wide wire; the cross section of the wire is $500 \times 1.2 \text{ nm}^2$. Walker breakdown is clearly visible for distinct values of DMI.

Both of the figures show analogous trend of the domain wall velocity; however, they have their differences. In figure 4-a-1, the domain wall velocity has been calculated for every 1mT increase in the external field while the same is not true in figure 4-a-2. This could

have contributed to some extent to the apparent differences. The size of the cross section of the modelled system was not identical; hence, it could have also influenced the outcome differently. In spite of some differences in the figures, the Walker breakdown velocity is approximately equal in both figures.

The simulation was continued for different values of DMI to observe the relationship between Walker field, Walker breakdown velocity, external field and DMI. The outcome is demonstrated in figure 4-b.

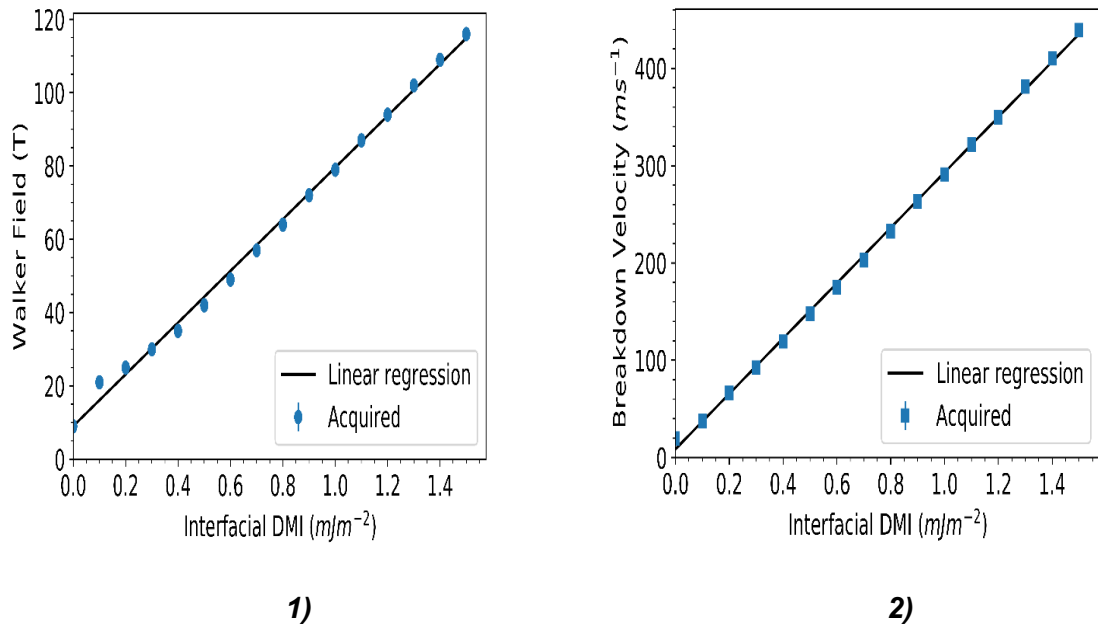


Figure 4-b: Relationship between interfacial DMI and 1) Walker field 2) Breakdown velocity.

It is evident from the figure 4-b that DMI prolongs the longevity of the stability of domain walls when they propagate. It can further be inferred from figure 4-b-1 that the Walker field increases linearly within the range of interest of this project. The Walker field increases by 70.54 T with every 1 mJm^{-2} increase in DMI. Breakdown velocity in figure 4-b-2 also shows a similar linear interdependence with interfacial DMI. The breakdown velocity increases by 284.37 ms^{-1} with every 1 mJm^{-2} increase in DMI. Another important observation is the anomaly stemming in figure 4-b-1. The Walker field value at 0.1 mJm^{-2} is clearly an offset from the linear trend. In order to further investigate the anomaly, it is necessary to observe the behaviour of domain wall velocity with respective DMI under the influence of external field.

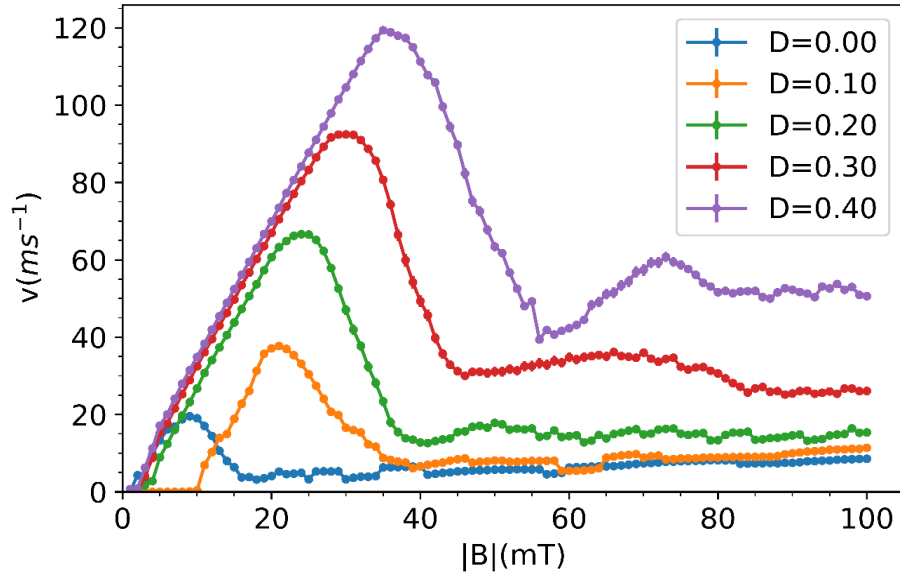


Figure 4-c: Domain wall velocity against the external magnetic field for five different DMI values including the anomalous value. The unit of D is mJm^{-2} .

The figure 4-c shows the behaviour of the domain wall velocity in response to external magnetic field focusing on the smaller values of DMI. The eccentric behaviour of domain wall velocity for $D = 0.10 \text{ mJm}^{-2}$ is immediately visible in figure 4-c. The velocity curve of $D = 0.10 \text{ mJm}^{-2}$ appears to have zero initial propagation velocity for specific amount of time contrary to the common linear trend being followed by other values of D . Additional simulations were done to understand this anomaly to a greater extent.

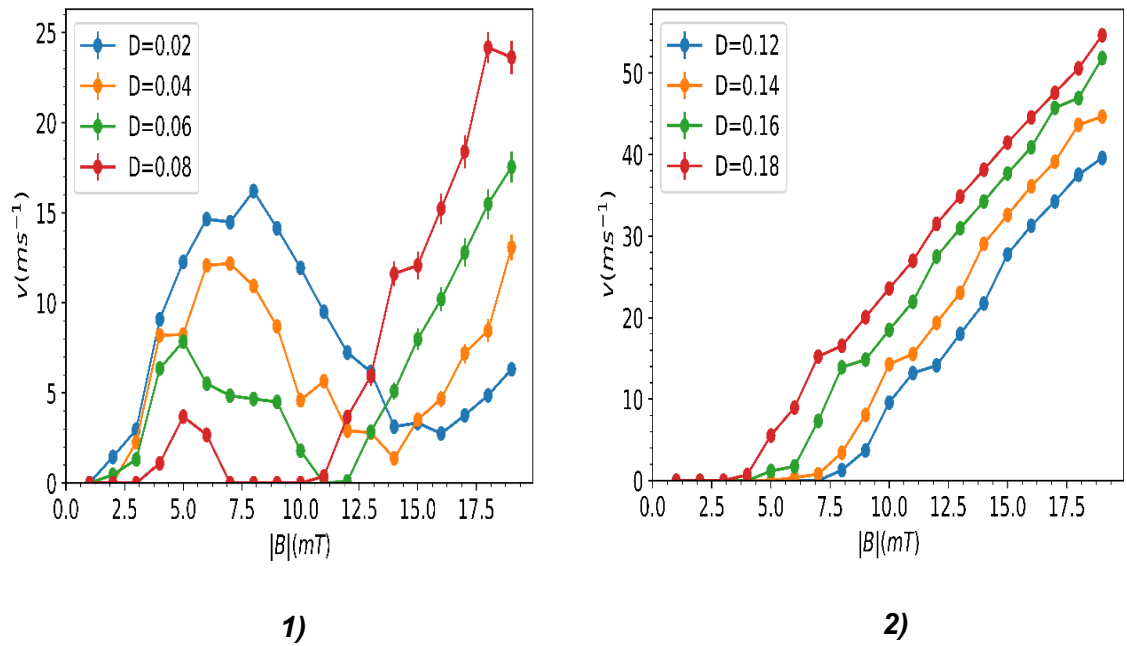


Figure 4-d: Domain wall velocity against external field for small DMI values, 1) below the anomalous value, 2) above the anomalous value. The unit of D is mJm^{-2} .

Figure 4-d-1 shows the result of DMI values less than 1.0 mJm^{-2} , whereas figure 4-d-2 illustrates the outcome for DMI values between 1.0 mJm^{-2} and 2.0 mJm^{-2} . In figure 4-d-1, the DMI appears to suppress the domain wall propagation instead of stabilizing it further. As the value of the DMI increases, the initial propagation of the domain wall gets further repressed leading to an apparent phenomenon similar to domain wall *pinning* and *depinning*.

The simulated system in this project is an ideal system with no sign of impurities. Existence of pinning and depinning-like phenomenon in this system would be very strange. The original behaviour of the domain wall position must be scrutinized to inspect this bizarre occurrence. A single field value was chosen from the corresponding range of irregularities and then new simulations were done using the field value. The run time of the simulations was also increased to observe any possible delays in the domain wall propagation.

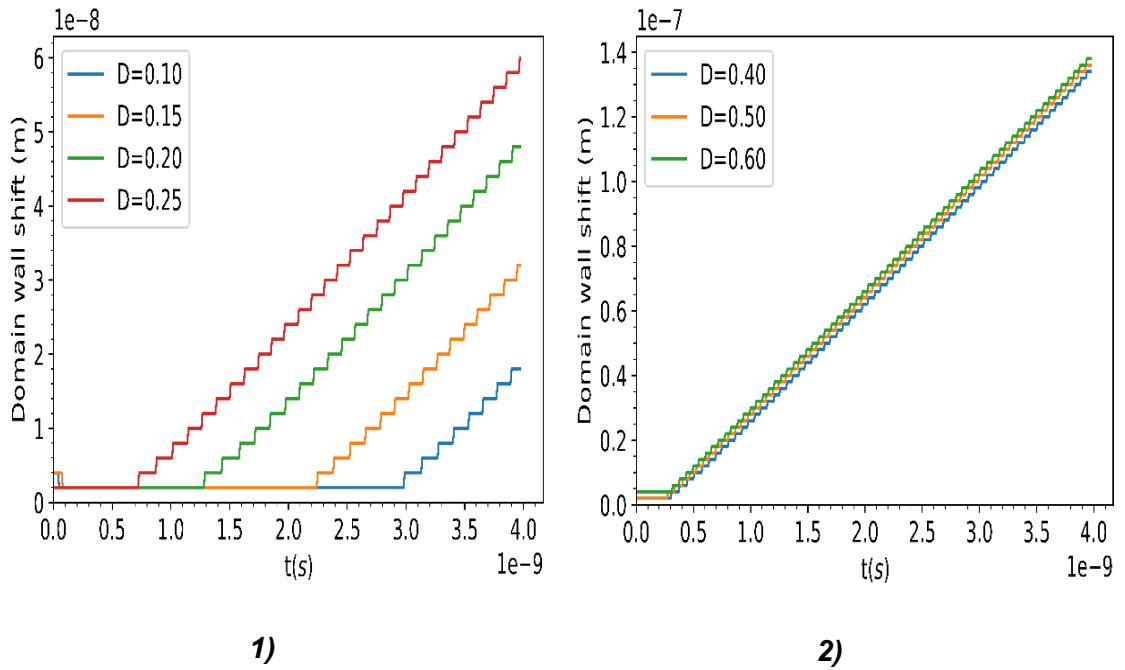


Figure 4-e: Domain wall position against elapsed time in magnetic field $|B| = 5.0 \text{ mT}$ for: 1) smaller values of DMI, 2) higher values of DMI. The unit of D is mJm^{-2} .

Figure 4-e shows the trend of domain wall position against elapsed time when an external field of magnitude 5.0 mT is applied to the system with different DMI values. Figure 4-e-1 helps understand the pinning and depinning-like phenomenon observed in figure 4-d. Smaller DMI values appear to affect the dynamics of domain wall differently than higher DMI values. The smaller DMI values take longer time before they favour the domain wall propagation. There exists a clear delay in the movement of the domain wall in lower values of DMI. Figure 4-e-2 shows the effect of higher DMI values in domain wall propagation. The initial delay with higher DMI values is much shorter.

All of the simulations previously performed had a run time of 1.5 ns; as a result, the strange phenomenon observed in figure 4-d is a consequence of the delay in the domain wall movement. Furthermore, figure 4-e-2 helps to validate the result obtained from simulations involving 1.5 ns run time. DMI values greater than 0.3 mJm^{-2} appear to have lower delay in the domain wall propagation and since the linear growth in the domain wall position is properly engulfed within the usual 1.5 ns run time of the simulation, the analyses of those simulations are still valid.

5. CONCLUSION

The effects of DMI on Walker breakdown was studied in the project through the means of micromagnetic simulation. The simulation was performed imitating a real experiment with genuine material parameters. Each simulation produced a data output and the output was further analysed. A thorough analysis of the data obtained from the simulation has led to the conclusion that DMI can play a crucial role in the stability of the domain walls. Magnetic domain walls can be stabilized to a greater extent under the influence of DMI. DMI defers the advent of the Walker breakdown and aids to attain higher domain wall velocity when exposed to external magnetic field. Substantial DMI value can also contribute in maintaining higher propagation velocity even after the Walker breakdown.

The breakdown velocity, within the range of interest of this study, increases linearly as the value of DMI increases. Identical trend follows in the case of the Walker field as well. The study also suggests that DMI can affect a system differently depending on its magnitude. When the value of DMI is very trace in a system exposed to smaller magnetic field, then there is a significant delay in the propagation of domain wall. On the contrary, higher DMI values have lower delays in the propagation of domain wall, regardless of the magnitude of external magnetic field.

This study has been done with limited resources and time. The objective of the project mainly focused on studying the relationship between interfacial DMI and Walker breakdown velocity within a smaller range of DMI values. The findings of the project are valid within the range being investigated however other ranges of DMI may influence the same system differently and hence is a topic of different research. The impact of the smaller value of DMI in the system was found very startling. A thorough research may be required to understand the phenomenon to a greater extent.

REFERENCES

- (magnetism 2019) 2019-last update. *magnetism*. [online]. Encyclopædia Britannica Inc. Available: <https://academic-eb-com.libproxy.tuni.fi/levels/collegiate/article/magnetism/106020> [10/04/2019].
- (Beach, Tsoi et al. 2008) BEACH, G.S.D., TSOI, M. and ERSKINE, J.L., 2008. Current-induced domain wall motion. *Journal of Magnetism and Magnetic Materials*, **320**(7), pp. 1272-1281.
- (Guimarães 2017) GUIMARÃES, A.P., 2017. *Principles of Nanomagnetism*. 2 edn. DE: Springer Verlag, pp. 1-14.
- (H. Föll 2018) H. FÖLL, 2018-last update, Domain Movement in External Fields. [online]. Available: https://www.tf.uni-kiel.de/matwis/amat/elmat_en/kap_4/backbone/r4_3_4.html [15/04/2019].
- (Hütner, Herranen et al. 2018) HÜTNER, J., HERRANEN, T. and LAURSON, L., 2018. Multistep Bloch-line-mediated Walker breakdown in ferromagnetic strips. arXiv preprint arXiv:1812.02545.
- (Mayergoyz, Bertotti et al. 2009) MAYERGOYZ, I.D., BERTOTTI, G. and SERPICO, C., 2009. *Nonlinear Magnetization Dynamics in Nanosystems*. GB: Elsevier Science, pp. 21-34.
- (Miyazaki, Jin 2013) MIYAZAKI, T. and JIN, H., 2013. *The Physics of Ferromagnetism*. 1. Aufl.; 2013 edn. Berlin, Heidelberg: Springer-Verlag, pp. 175-286.
- (Mougin, Cormier et al. 2007) MOUGIN, A., CORMIER, M., ADAM, J.P., METAXAS, P.J. and FERRE, J., 2007. Domain wall mobility, stability and Walker breakdown in magnetic nanowires, arXiv:cond-mat/0702492 [cond-mat.mtrl-sci].
- (Skomski 2010) SKOMSKI, R., 2010. *Simple Models of Magnetism*. GB: Oup Oxford, pp. 1-14.
- (Vansteenkiste, Leliaert et al. 2014) VANSTEENKISTE, A., LELIAERT, J., DVORNIK, M., HELSEN, M., GARCIA-SANCHEZ, F. and VAN WAEYENBERGE, B., 2014. The design and verification of MuMax3. *AIP Advances*, **4**(10), 107133.
- (Yoshimura, Kim et al. 2016) YOSHIMURA, Y., KIM, K., TANIGUCHI, T., TONO, T., UEDA, K., HIRAMATSU, R., MORIYAMA, T., YAMADA, K., NAKATANI, Y. and ONO, T., 2016. Soliton-like magnetic domain wall motion induced by the interfacial Dzyaloshinskii-Moriya interaction. *Nature Physics*, **12**(2), pp. 157-161.